Biosensors and Bioelectronics 57 (2014) 41–47

Contents lists available at ScienceDirect

Biosensors and Bioelectronics

journal homepage: www.elsevier.com/locate/bios

Multianalyte electrochemical biosensor on a monolith electrode by optically scanning the electrical double layer

Seung-Woo Lee, Ravi F. Saraf*

Department of Chemical and Biomolecular Engineering, University of Nebraska-Lincoln (UNL), 207 Othmer Hall, Lincoln, NE 68588-0643, USA

ARTICLE INFO

Article history:
Received 5 November 2013
Received in revised form
12 January 2014
Accepted 23 January 2014
Available online 2 February 2014

Keywords:
Multianalyte sensor
Electrochemical sensor
Biosensor
Electrical double layer
Microarray
Differential interferometer

ABSTRACT

Redox on an electrode is an interfacial phenomenon that modulates the charge in the electrical double layer (EDL). A novel instrument, the Scanning Electrometer for Electrical Double-layer (SEED) has been developed to measure multiple enzyme reactions on a monolith electrode due to immunospecific binding with a mixture of respective analytes. SEED quantitatively maps the local redox reaction by scanning a laser on the array of enzyme monolayer spots immobilized on the monolith electrode. SEED measures the change in local charge state of the EDL that abruptly changes due to the redox reaction. The measurement spot size defined by the size of the laser beam is ~10 μm. The SEED signal is linearly proportional to the local redox current density and analyte concentration. The specificity is close to 100%. The SEED readout is compatible with microfluidics platform where the signal degrades less than 2% due to the poly(dimethyl siloxane) (PDMS) body.

1. Introduction

Amperometric measurement of redox current on immunospecific binding of analyte with immobilized monolayer of enzyme on an electrode has revolutionized chemical sensor industry. The electrochemical detection of analytes at high sensitivity and selectivity using "enzyme electrodes" has had great success as biosensors during the past few decades(Wang, 2008). For example, the glucometer, is arguably the most successful chemical sensor in history, detecting glucose via immunospecific binding to glucose oxidase (GOx) immobilized on an electrode. (Newman and Turner, 2005; Yoo and Lee, 2010). Enzyme electrodes (also referred to as wired enzymes) were first demonstrated over three decades ago, (Eddowes and Hill, 1977; Yeh and Kuwana, 1977) disproving the dogma that a mediator is necessary to electrochemically couple an enzyme to an electrode. Since then, many strategies have been developed to wire the enzyme using a variety of promoters, (Hu, 2001) such as conducting polymer, (McQuade et al., 2000; Ramanavicius et al., 1999) metal cations, (Armstrong et al., 1984) and nanomaterials. (Jacobs et al., 2010; Mano and Heller, 2005; Mao et al., 2003; Willner et al., 2006). Elegant interface chemistries are developed by incorporating the enzyme into conducting polymer media with a redox center tethered to the polymer chain to effectively collect the redox electrons. (Mano and Heller, 2005; Mao et al., 2003) In a remarkable study, a ~2 nm Au nanoparticle was "imbedded" directly into GOx to wire the active site of the enzyme to the electrode. (Xiao et al., 2003) Another highly versatile, scalable method is the layer-by-layer assembly of polyelectrolytes incorporating, moderators and promoters (such as nanoparticles, enzymes, nanomaterials). (Calvo et al., 2000; Zhao et al., 2006) The conduction occurs due to the ionic nature of the polyelectrolytes.

With the success of the single analyte electrochemical biosensors, multiplexing and miniaturization are natural extensions. One of the most pervasive ideas has been to measure a signal in an indirect electrochemical event. The first combinatorial electrochemistry example was to study catalytic action of a combination of five metals to optimize an electrode for fuel cells (Reddington et al., 1998). The level of redox activity was measured as a fluorescent signal from the redox product. For large-scale multiplexing, the most successful approach has been to translate complementary metal-oxide semiconductor (CMOS) technology. In one chip, an antibody-antigen addressable sensor array has been designed using an enzyme-labelled target to generate a redox signal (Dill et al., 2004; Ghindilis et al., 2007). The approach is further modified by incorporating a small redox molecule (i.e., PQQ) at the electrode surface to enhance the signal (Polsky et al., 2008). Recently, in a remarkable approach, an electrochemical DNA sensor was designed where modulation in the pH due to (local) polymerase-based synthesis of DNA on a probe template is measured on each pixel as a change in current (Rothberg et al., 2011). The local pH change modulates the gating potential. However, in multianalyte detection biosensor, array of individual microelectrode for each analyte with corresponding

* Corresponding author. Tel.: +1 402 472 2750; fax: +1 402 472 6989.
E-mail addresses: rsaraf@unlnotes.unl.edu, rsaraf@unlnotes.unl.edu (R.F. Saraf).

http://dx.doi.org/10.1016/j.bios.2014.01.043
0956-5663

(immobilized) enzyme needs to be fabricated (Wilson and Nie, 2006; Yan et al., 2010). The number of sensing electrodes in the array have to be equal to the number of analytes to be tested, with additional counter and reference electrodes for each sensing electrode (depending on the design). The electrical isolation of the individual electrode in the microarray to reduce noise due to coupling adds complexity and cost to the design which remains a challenge (Ebrahimi et al., 2008). Furthermore, the redox current monotonically reduces as the sensor electrode size diminishes.

Here, we describe a novel laser scanning method to quantitatively address multiple redox reactions on a monolith electrode with a microarray of immobilized enzymes. The laser beam measures the local redox reaction on the enzyme spot by measuring the charge state of the electrical double layer (EDL) (Singh and Saraf, 2006). The EDL charge abruptly changes at the redox potential and the change in charge (compared to equilibrium state) is linearly proportional to the redox current density. Thus, the optical signal is linearly proportional to the local redox current density on the ~10 μm laser spot and the analyte concentration. The method is called a Scanning Electrometer for Electrical Double-layer (SEED).

2. Material and methods

In this section, the principle of SEED is briefly described; followed by surface modification and immobilization of enzyme to fabricate the enzyme chip; and lastly the method of SEED measurement is described.

2.1. Scanning electrometer for electrical double-layer (SEED)

The principle of SEED is described in a previous publication (Singh et al., 2009). To facilitate the interpretation of the results and discussion, the basic principle of SEED is briefly outlined. Two orthogonally polarized laser beams, having the same intensity, were incident onto the SU-8 patterned monolith working electrode (WE) that has the immobilized enzymes. The probe beam is on the sensing site while the reference beam is on the WE that is coated with SU-8 (Fig. 1(a) and Fig. A in Supplementary data Information (SI)). The pair of beams is scanned spot-to-spot over various enzyme sites (Fig. 1(a)). Fig. 1(b) shows a photograph of the actual SEED apparatus. In a typical electrochemical experiment, a periodic bias, V_{DC}, at a frequency of 20 mHz from -200 mV to 800 mV is applied between the WE and the reference electrode (RE) by a potentiostat; and the redox current is measured between the CE and the WE. The RE is a standard Ag/AgCl electrode, and CE is Pt wire. Additionally, a 50 mV AC potential ($\omega \sim 2$ kHz) is applied on the WE to produce an optical signal described next. The AC potential will oscillate the ions in the vicinity of the electrode (within 100 nm as described in the next paragraph) to cause a periodic modulation of the ion concentration at ω. The concentration modulation will result in oscillation in the path length. This amplitude of the path length oscillation is measured by differential interferometer as an optical signal, Δ (SI, Fig. A). Because the reference beam (incident on the passivated part of the electrode with no electrochemical activity) and the probe beams are always only ~100 μm apart (see microscope image in Fig. 3(a, inset) to be discussed later), the thermal noise is greatly reduced resulting in highly stable optical signal at pico-meter (pm) sensitivity (Fig. B, SI). To note is that the three electrodes, WE, RE and CE are controlled by a potentiostat to concomitantly acquire both optical (SEED) and cyclic voltammetry (CV) data.

The nature the optical signal, Δ, is considered. As the WE comes into contact with the electrolyte solution, an EDL is spontaneously formed. The thickness of the EDL is $\sim 10\,\zeta$, where ζ is the Debye length, which is inversely proportional to the square root of ion concentration. Typically, for a 100 mM solution, ζ is ~1 nm (Israelachvili, 1992). Due to the ion accumulation in the EDL, the electric field emanating from the WE is screened within $\sim 10\zeta$. (Torrie and Valleau, 1979) Thus, for 100 mM solutions, the ion oscillation due to the AC potential applied on the WE is limited to well within ~15 nm. When the V_{DC} ramp cycle is close to the redox potential, E°, there is a large amount of electron exchange between the WE and the redox ions in the EDL leading redox current. As the ion diffusion in response to charge imbalance is significantly slower than the rapid electronic exchanges between the redox ion and the WE, the electrostatic screen due to an EDL charge is significantly diminished. As a result, the AC field emanating from the WE will penetrate deeper into the electrolyte solution during redox, resulting in an increase in ion oscillation at the interface. As a result, Δ is maximum, Δ_{max}, close to the redox potential, commensurate with the redox current (Fig. B, SI). From Gauss's law, for a planar electrode (i.e., one-dimensional system), the increase in electric field due to descreening is linearly proportional to the magnitude of charge imbalance (Xiao et al., 2003). As the charge imbalance is proportional to the redox current (for a fixed V_{DC} ramp rate), the increase in the magnitude of the electric field is linearly proportional to the redox current. Thus, the optical signal at redox, Δ_{max}, is linearly proportional to the local redox current density, I_{max}, averaged over the 10 μm laser spot (see inset of Fig. B, SI). Owing to linear proportionality between Δ_{max} and I_{max}, SEED quantitatively measures the local redox current density. Furthermore, because I_{max} is proportional to analyte concentration, Δ_{max} is expected to be linearly proportional to analyte concentration. The linearity is explicitly shown in Fig. 4.

If the solution contains only glucose at the redox potential, a large AC field penetration occurs on the spot with GOx at the redox potential (leading to Δ_{max}), as schematically shown in Fig. 1 (a). The oscillation over the other two spots with GalOx and AlOx will not have any significant increase Δ as the V_{DC} is ramped over the redox potentials for all of the enzymes.

2.2. Device fabrication

Three polygonal openings on a gold WE (1 mm(W) × 10 mm(L)) were fabricated by a UV-lithographic method on 50 μm thick SU-8 film (Fig. 2(a)). The sensing side is at the apex of the isosceles triangle, which is ~600 μm long; and the apex angle is ~45°. The broad rectangular-like shape facilitated immobilization of the enzyme at the apex by surface tension (i.e., wicking). The SEED measurement was performed at the apex to take advantage of signal enhancement due to (dielectrophoretic) electric field focusing caused by the surrounding SU-8 (Lee et al., 2013). The probing at the apex also demonstrated the feasibility of the possible measurement spot size of ~10 μm by SEED. After O_2 plasma for 1 min., the device was spin-coated with alternating ~0.9 nm thick layers of PAH (3 mg/ml, 15,000 Da, Sigma Aldrich) and PSS (3 mg/ml, 70,000 Da, Sigma Aldrich) at 3000 rpm. The GOx, GalOx (galactose oxidase), and AlOx (alcohol oxidase) in 10 mM phosphate buffer saline (PBS, pH.~7.4) were locally micro-pipetted at the larger side of the pattern for immobilization (Fig. 2(b)). To immobilize GOx and AlOx, three layers of PAH/PSS/PAH were deposited. For GalOx, only PAH/PSS was deposited such that the top layer was negatively charged (i.e., PSS). The solution was wicked over the opening due to the hydrophilic nature of the surface caused by polyelectrolyte coating. The 50 μm thick SU-8 film confines the enzyme solution droplet over the electrode opening. The device was stored overnight at 4 °C to ensure complete (saturated) immobilization of the enzyme. The device was gently washed with 10 mM PBS, and the other PAH/PSS layers were spin-coated to encapsulate three immobilized enzymes.

2.3. SEED measurement

The analyte solutions with substrates (glucose, galactose, and alcohol (ethanol)) were prepared in 10 mM sodium phosphate buffer with 10 mM NaCl (pH.7.4–7.5). The measurement was performed in two configurations. In the first configuration, the device was placed in a home-built plastic (Upilex®) electrochemical chamber with a quartz glass window to allow the lasers to enter (Figs. 1 and 3(a)). The Ag/AgCl reference electrode (3 M KCl, Warner Instrument, Co.) and Pt wire (dia.~10 μm), as a CE, were inserted into the electrochemical chamber. The probe beam was at the corner of an isosceles triangle, while the reference beam was placed on SU-8 passivation film (Fig. 3(a, inset)). In the second configuration, the device was incorporated into a microfluidics channel (Fig. 3(b)). A 700 μm (W) × 8 mm (L) × 100 μm (H) channel was molded into a PDMS (Sylgard 184) film of ~2 mm thickness. The mold is placed over the device with the three enzymes immobilized on the WE (Fig. 3(b, inset)). The platinum CE wire and the Ag/AgCl RE were inserted at the two ends of the PDMS channel. The three enzyme electrodes in the device are (easily and) conveniently scanned through transparent PDMS film under the same conditions as the electrochemical chamber experiment with the beam at the apex of the triangle.

As described in the above section on SEED, if glucose is present in the solution, a Δ_{max} will be observed only on the spot with immobilized GOx. The selectivity and sensitivity of the various analytes on the enzyme spots; and the sensitivity is discussed in the next Section. For the study, Δ_{max} was averaged over five V_{DC} ramp cycles to compute the error bars (see for example Fig. F–I in SI to be discussed later in more details).

3. Results and discussion

3.1. Sensitivity

The optical signal from SEED was compared to the concomitantly obtained redox current (i.e., CV) to compare the two methods and interpret the results. The general nature of the redox signal for all the three enzymes was similar. The redox of glucose

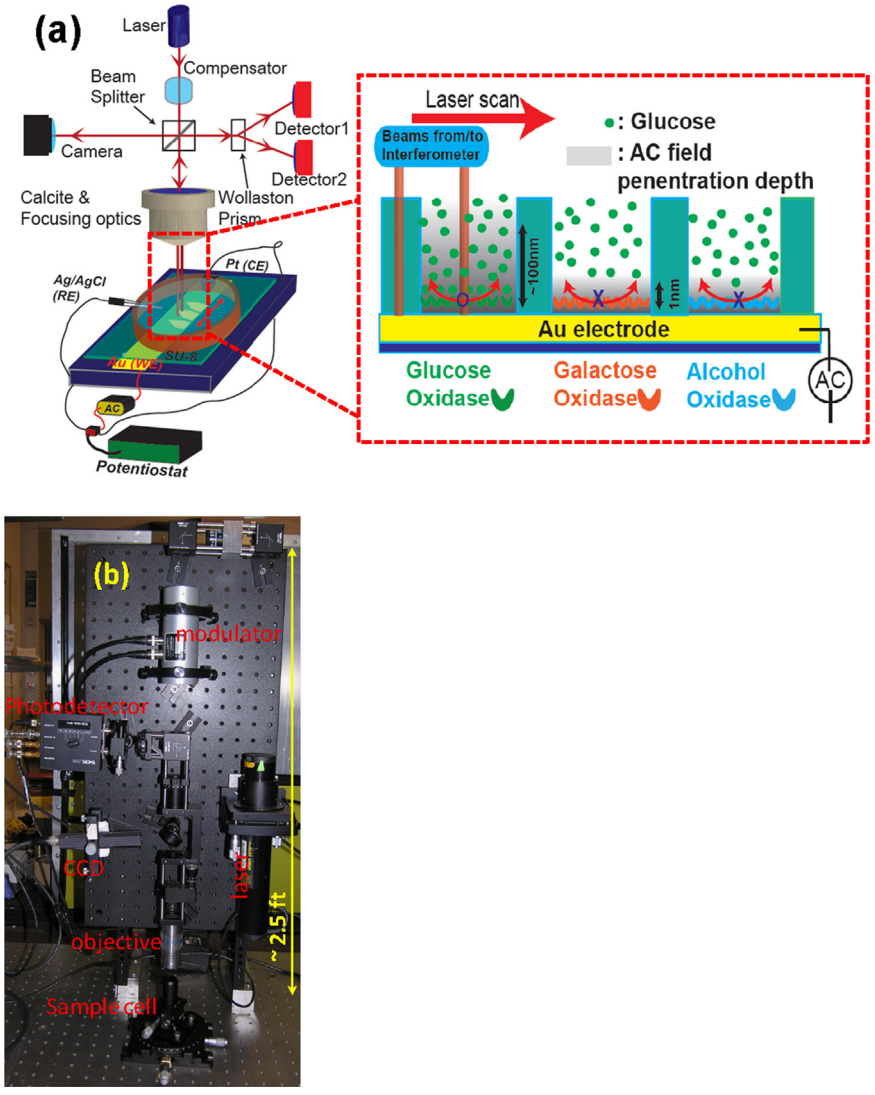

Fig. 1. SEED measurement concept (a) Schematic measurement concept of SEED for a three-enzyme microarray. Two laser beams with the same intensity were incident on the immobilized enzyme spot and the electrode passivated with SU-8. All of the enzymes were immobilized on a monolith underlining a gold electrode. A 50 mV amplitude AC potential at ω ~2 kHz was applied on the sensing (i.e., working) electrode to produce the SEED signal. (Inset depicts the EDL modulation the redox potential. The solution is assumed to have only glucose, thus the reaction exclusively occurred only on the GOx spot due to immunospecific binding. As a result, the AC field penetrated deeper into the solution at the redox potential to cause an increase in the SEED signal on GO*x*, while AC penetration on GalOx and AlO*x* sites does not change significantly) (b) Photograph of the SEED apparatus showing the salient components.

mediated by GO*x* is considered as an example. The CV of 100 mM glucose on GO*x* immobilized enzyme electrode shows a reduction and oxidation peaks at, ~260 mV and ~400 mV (Fig. 4(a)). For the electrode size used in the study, a large concentration of glucose was necessary to obtain a good quality CV signal. The oxidation peak corresponds to formal potential for conversion of H_2O_2 to O_2 at ~450 mV (Gerlache et al., 1997). The flavin adenine dinucleotide (FAD) was reduced to $FADH_2$ in the reduction cycle which can span ~250 mV around the formal potential at 0 mV, due to environmental effects, especially the positive charge surrounding the protein (Mattevi, 2006). The optical signal (i.e., Δ_{max}) was consistent with the CV (i.e., I_{max}). More importantly, as discussed above, Δ_{max} was linearly proportional to concentration (Fig. 4(b)). It is important to note that a finite Δ_{max} is measured at glucose concentration of 0 mM. The background signal at 0 mM analyte concentration, Δ_B=5.3 pm, is due to the nonturnover redox of GOx.

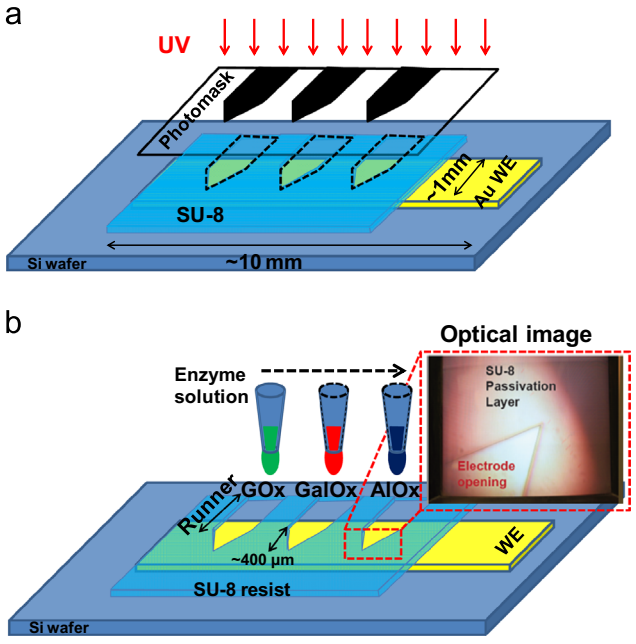

Fig. 2. Device fabrication steps (a) Schematic showing a single-step photolithographic process which can fabricate three different zones for each enzyme on a single monolith Au WE. (b) Individual enzyme solution is placed on a runner track of each spot, and wicked to the triangle electrode opening. (Inset : A microscope image showing the electrode opening surrounded by the SU-8 passivation layer).

As the enzyme flip-flopped between the two redox states, FAD and $FADH_2$, the EDL charge imbalance led to Δ_{max} due to the oscillation of the ions in the buffer solution. To note is that Δ_B had little variation from sample-to-sample. The Δ_B primarily depended on the extent of coverage which is close to saturation for all the samples. The individual scans for various concentrations are shown in Fig. C., SI. Similar to GO*x*, other enzymes also exhibited a linear behaviour (Fig. 4(c and d)). The corresponding scans from SEED for other analyte/enzyme combinations are shown in Fig. C–E, SI. From the slope, the activity of GalO*x* was about five times higher than the other two enzymes.

3.2. Specificity

To study the selectivity of the enzyme chip, three solutions of 10 mM glucose, 2 mM galactose, or 10 mM alcohol on the three enzyme sites were studied by scanning. The solutions were injected into the plastic sample chamber (Fig. 3(a)). The optical scan on each spot was obtained by scanning the pair of laser beams (Fig. 5(a)). The CV signal was an integrated signal over all three sites, thus we do not have any information on the characteristics of the three individual enzyme electrodes. The optical signals (raw data) for the five scans measured on each spot are shown in Figs. F–H in SI for each of the three solutions. The corresponding Δ_{max} for each of the five scans on each spot, based on the raw data in SI, clearly showed high specificity (Fig. 5(b–d)). For example, for the 10 mM glucose solution (Fig. 5(b)), the signal, Δ_{max} on GOx spot is well above the background, Δ_B. The signal is consistent with the sensitivity curve for 10 mM glucose (in Fig. 4(b)). The Δ_B for each enzyme (from Fig. 4) is shown as a blue data point in Fig. 5(b–d). For the signal on the other two spots, i.e., GalOx and AlOx spots, Δ_{max} is Δ_B, which is consistent with 0 mM concentration of galactose and alcohol, respectively. The spot-to-spot Δ_{max} characteristics for the 2 mM galactose and 10 mM alcohol solution in Fig. 5(c and d), respectively, exhibited similar specificity as the glucose solution described above. The signal above the background for "active" spots and equal to Δ_B for "inactive" spots, which are quantitatively consistent with the sensitivity line in Fig. 4, indicates that SEED can detect multianalyte on a monolith electrode. As the SEED signal (above Δ_B) occurs due to an (active) bioelectrochemical redox reactions and is virtually blind to nonspecific binding, the specificity of the enzyme based multianalyte system is 100%.

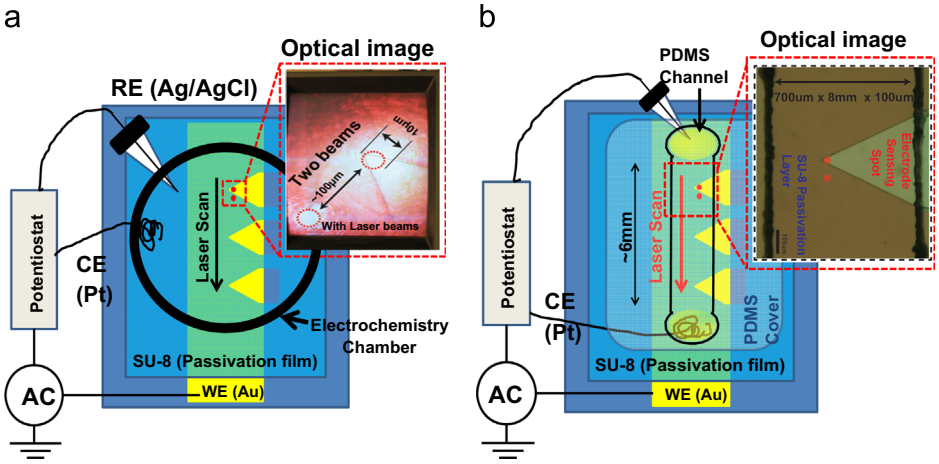

Fig. 3. SEED measurements. After enzymes are immobilized on the three spots, the device was tested in two different environments, in an electrochemical cell (a) and in a PDMS based microfluidic channel (b). Inset of (a) showing two SEED beams placed on an electrode opening and the SU-8 passivation layer. A microscope image (Inset of (b)) showing the PDMS microfluidic channel placed on a gold electrode.

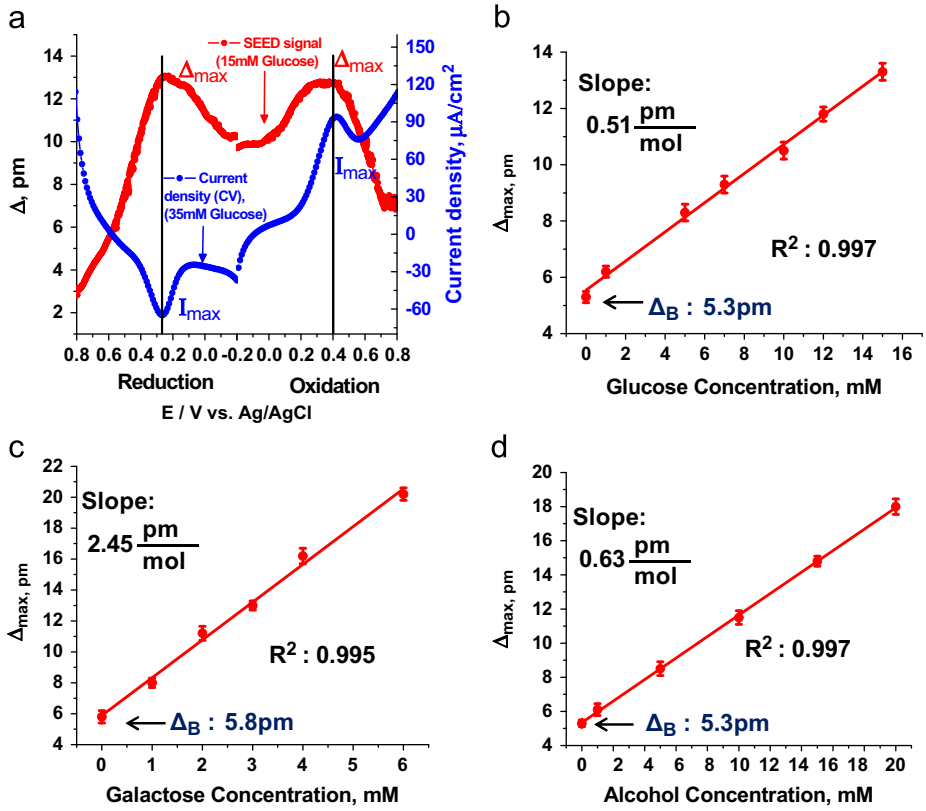

Fig. 4. SEED signal for individual enzymes immobilized on a Au electrode (a) Typical SEED signal from GOx immobilized on a Au electrode in 15 mM Glucose. The potential at maximum optical signal from SEED, Δ_{max}, and current from a potentiostat, I_{max}, were consistent for both the oxidation and reduction processes. (b) The Δ_{max} due to redox on GOx in a glucose solution (similar to (a)) as a function of concentrations showed a linear relationship. (c) and (d) similar to (b), the study is for GalOx, and AlOx enzymes in a corresponding analyte solution, respectively. The finite optical signal, Δ_B at 0 mM substrate concentration, was due to nonturnover redox of the enzyme. Each data point averaged over five ramp cycles. The average error bars were within 0.4 pm.

3.3. *Multiple analyte detection and microfluidics platform*

Two different mixtures with all of the three analytes were tested. The first mixture was a "high-risk case" (green line in Fig. 6). For the high-risk case, all three substrates were in abnormal ranges. The mixture contained 10 mM glucose (normal range ~4–7 mM (Kentrup et al., 1999; Wang, 2008)), 6 mM galactose (normal range ~0.5–1 mM (Kentrup et al., 1999)), and 15 mM alcohol (~legal limit in the U.K. (Albalate, 2008)). For the green curve, the Δ_{max} of 10.5 pm on a GOx spot, 19.8 pm on a GalOx spot, and 14.6 pm on an AlOx spot were consistent with the sensitivity curve in Fig. 4. The second mixture was for a "low-risk case," where glucose and galactose are in normal range; but the alcohol was above 0 mM (blue line in Fig. 6). The low-risk case mixture contained 10 mM alcohol (~0.05% BAC (blood alcohol contents)), 5 mM glucose, and 1 mM galactose. The corresponding signal of Δ_{max} of 8.5 pm for glucose, 8.1 pm for galactose, and 11.3 pm for alcohol was consistent with the sensitivity line in Fig. 4. The chip with the three enzyme electrodes was covered with a microfluidics channel with RE and CE at the two ends of the channel (Fig. 3(b)). The fabrication steps of the microfluidic channel is briefly described in Fig. L in SI. The enzyme electrode was clearly visible through the transparent PDMS mold (optical image in Fig. 3(b)). The coloring of the various regions in the optical image is due to thickness contrast. Only the triangular portion of the electrode is onside the 700 μm wide channel. The two red dots were false spots indicating the location of the laser beam. The spots were well defined and sharp indicating the scattering due to PDMS structure is insignificant. The signal for the high-risk case from the microfluidics channel (red curve in Fig. 6) was consistent with the response from the sample chamber (green curve). The characteristics for the high-risk samples are within 2% of the data obtained from the sample chamber where scattering and multiple reflection effects are minimal. The high consistency observed demonstrated that SEED can measure multiple enzyme reactions on a single monolith WE on a microfluidics platform.

4. Conclusion

In summary, we described multianalyte detection on a monolith electrode using a novel optical tool, SEED, that can quantitatively read individual redox reactions on an array of immobilized enzyme by spot-to-spot scanning of a probe laser. SEED is a differential interferometer where the (local) sensing was performed by scanning a pair of ~10 μm diameter laser beams over the sensing electrode. The central principle of SEED is to measure the modulation in the relative charge in the EDL which is extreme at the redox potential. For planar electrode, the signal at the redox potential scales linearly with the analyte concentration and the redox current density.

The microarray chips for SEED, with electrochemically active enzyme spots, were made by conventional lithography where the resist served as both a passivation layer for the reference beam and a layer to focus the electric field to enhance the (redox) signal. The signal is highly specific to the substrate–enzyme binding. Because the signal was produced due to the active process of bioelectrochemical redox reactions, SEED was blind to nonspecific reactions. In the absence of the substrate, a constant background signal was produced due to the nonturnover redox of the enzyme. Because the optical signal is linearly proportional to the measured

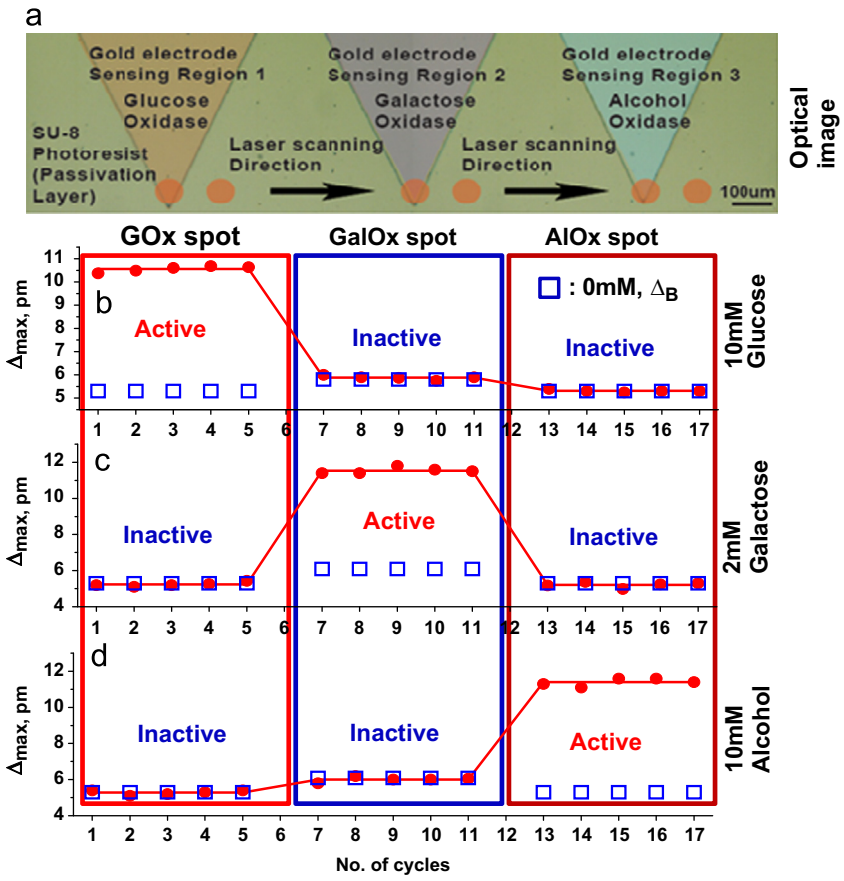

Fig. 5. Selectivity assessment of the enzyme array chip (a) Optical microscope image showing three designed sensing spots surrounded by 50 μm thick SU-8 resist. The false coloring on the three sensing spots is to show the structure of the array which has three different enzymes, as ladled over each triangular spot. The red dot is schematically drawn to depict the location and relative size of the 10 μm diameter laser spots from SEED. (b) The optical signal (i.e., Δ_{max}) from SEED in 10 mM glucose is shown filled with (red) circles. As expected, only the spot with immobilized GOx is "active" with a $\Delta_{max} \sim 10.5$ pm, while the other two spots are "inactive" where the $\Delta_{max} = \Delta_B$. The five data points for each spot corresponded to different V_{DC} ramp cycles. (c) and (d) similar to (b), the study is for 2 mM galactose and 10 mM alcohol solution, respectively. As a reference, the data points with open (blue) square correspond to Δ_B measured on single enzyme electrode (in Fig. 4). (For interpretation of the references to color in this figure legend, the reader is referred to the web version of this article.)

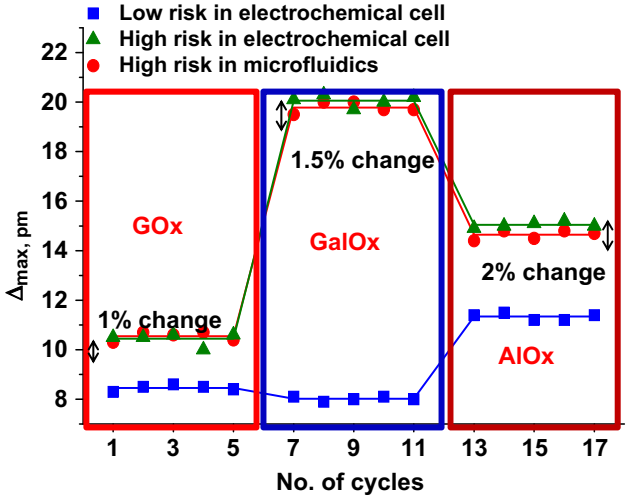

Fig. 6. Response from enzyme microarray in a microfluidics channel Optical response on each spot for low-risk (blue line) and high-risk (green line) solutions measured in a sample chamber similar to Fig. 5. All of the three spots are active. The data points correspond to Δ_{max} measured during (the five) individual V_{DC} ramp cycles. The red line with corresponding data points of the same color indicate the response from a high-risk solution in the microfluidics channel.(For interpretation of the references to color in this figure legend, the reader is referred to the web version of this article.)

the analyte concentration, SEED quantitatively analyzes multi-analyte mixtures. The relevant concentration range for a mixture of three analytes, glucose, galactose and alcohol, on an enzyme array (corresponding to three substrates) was studied to demonstrate the principle and feasibility of SEED as a tool for practical application. The ability to read local redox on a monolith electrode with an array of electrochemically active probes by simple laser scanning opens the possibility of using SEED to read electrochemical chips for combinatorial and microarray analysis where the signal is blind to nonspecific binding. SEED is compatible with a microfluidics platform.

Acknowledgment

R.F.S. would like to thank the National Science Foundation (CBET- 7389730) and the Nebraska Tobacco Funds for their financial support.

Appendix A. Supporting information

Supplementary data associated with this article can be found in the online version at http://dx.doi.org/10.1016/j.bios.2014.01.043.

References

Albalate, D., 2008. J. Policy Anal. Manage. 27, 20–39.
Armstrong, F.A., Hill, H.A.O., Oliver, B.N., Walton, N.J., 1984. J. Am. Chem. Soc. 106, 921–923.
Calvo, E.J., Battaglini, F., Danilowicz, C., Wolosiuk, A., Otero, M., 2000. Faraday Discuss. 116, 47–65.
Dill, K., Montgomery, D.D., Ghindilis, A.L., Schwarzkopf, K.R., Ragsdale, S.R., Oleinikov, A.V., 2004. Biosensens. Bioelectron. 20, 736–742.
Ebrahimi, D., Chow, E., Gooding, J.J., Hibbert, D.B., 2008. Analyst 133, 1090–1096.
Eddowes, M.J., Hill, H.A.O., 1977. J. Chem. Soc. Chem. Commun., 771–772
Gerlache, M., Senturk, Z., Quarin, G., Kauffmann, J.M., 1997. Electroanalysis 9, 1088–1092.
Ghindilis, A.L., Smith, M.W., Schwarzkopf, K.R., Roth, K.M., Peyvan, K., Munro, S.B., Lodes, M.J., Stover, A.G., Bernards, K., Dill, K., McShea, A., 2007. Biosens. Bioelectron. 22, 1853–1860.
Hu, N.F., 2001. Pure Appl. Chem. 73, 1979–1991.
Israelachvili, J., 1992. Intermolecular and Surface Forces. Academic Press Limited, London
Jacobs, C.B., Peairs, M.J., Venton, B.J., 2010. Anal. Chim. Acta 662, 105–127.
Kentrup, H., Altmuller, J., Pfaffle, R., Heimann, G., 1999. Eur. J. Endocrinol. 1999/10/20, 379–381.
Lee, S.-W., Lopez, J., Saraf, R.F., 2013. Biosens. Bioelectron. 47, 408–414.
Mano, N., Heller, A., 2005. Anal. Chem. 77, 729–732.
Mao, F., Mano, N., Heller, A., 2003. J. Am. Chem. Soc. 125, 4951–4957.
Mattevi, A., 2006. Trends Biochem. Sci. 31, 276–283.
McQuade, D.T., Pullen, A.E., Swager, T.M., 2000. Chem. Rev. 100, 2537–2574.
Newman, J.D., Turner, A.P.F., 2005. Biosens. Bioelectron. 20, 2435–2453.
Polsky, R., Harper, J.C., Wheeler, D.R., Brozik, S.M., 2008. Electroanalysis 20, 671–679.
Ramanavicius, A., Habermuller, K., Csoregi, E., Laurinavicius, V., Schuhmann, W., 1999. Anal. Chem. 71, 3581–3586.
Reddington, E., Sapienza, A., Gurau, B., Viswanathan, R., Sarangapani, S., Smotkin, E. S., Mallouk, T.E., 1998. Science 280, 1735–1737.
Rothberg, J.M., Hinz, W., Rearick, T.M., Schultz, J., Mileski, W., Davey, M., Leamon, J.H., Johnson, K., Milgrew, M.J., Edwards, M., Hoon, J., Simons, J.F., Marran, D., Myers, J. W., Davidson, J.F., Branting, A., Nobile, J.R., Puc, B.P., Light, D., Clark, T.A., Huber, M., Branciforte, J.T., Stoner, I.B., Cawley, S.E., Lyons, M., Fu, Y.T., Homer, N., Sedova, M., Miao, X., Reed, B., Sabina, J., Feierstein, E., Schorn, M., Alanjary, M., Dimalanta, E., Dressman, D., Kasinskas, R., Sokolsky, T., Fidanza, J.A., Namsaraev, E., McKernan, K.J., Williams, A., Roth, G.T., Bustillo, J., 2011. Nature 475, 348–352.
Singh, G., Moore, D., Saraf, R.F., 2009. Anal. Chem. 81, 6055–6060.
Singh, G., Saraf, R.F., 2006. J. Phys. Chem. B 110, 12581–12587.
Torrie, G.M., Valleau, J.P., 1979. Chem. Phys. Lett. 65, 343–346.
Wang, J., 2008. Chem. Rev. 108, 814–825.
Willner, B., Katz, E., Willner, I., 2006. Curr. Opin. Biotechnol. 17, 589–596.
Wilson, M.S., Nie, W.Y., 2006. Anal. Chem. 78, 2507–2513.
Xiao, Y., Patolsky, F., Katz, E., Hainfeld, J.F., Willner, I., 2003. Science 299, 1877–1881.
Yan, J., Pedrosa, V.A., Simonian, A.L., Revzin, A., 2010. ACS Appl. Mater. Interfaces 2, 748–755.
Yeh, P., Kuwana, T., 1977. Chem. Lett. 6, 1145–1148.
Yoo, E.H., Lee, S.Y., 2010. Sensors (Basel) 10, 4558–4576.
Zhao, W., Xu, J.J., Chen, H.Y., 2006. Electroanalysis 18, 1737–1748.